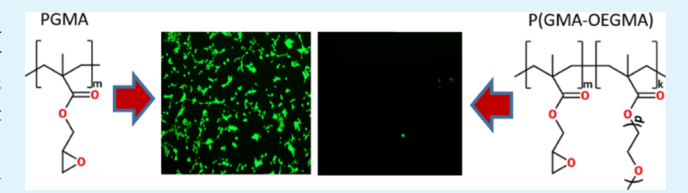
En Route to Practicality of the Polymer Grafting Technology: One-Step Interfacial Modification with Amphiphilic Molecular Brushes

Nikolay Borodinov, ** Dmitry Gil, ** Mykhailo Savchak, ** Christopher E. Gross, * Nataraja Sekhar Yadavalli, Ruilong Ma, Vladimir V. Tsukruk, Sergiy Minko, Alexey Vertegel, and Igor Luzinov*,†®

Supporting Information

ABSTRACT: Surface modification with polymer grafting is a versatile tool for tuning the surface properties of a wide variety of materials. From a practical point of view, such a process should be readily scalable and transferable between different substrates and consist of as least number of steps as possible. To this end, a cross-linkable amphiphilic copolymer system that is able to bind covalently to surfaces and form



permanently attached networks via a one-step procedure is reported here. This system consists of brushlike copolymers (molecular brushes) made of glycidyl methacrylate, poly(oligo(ethylene glycol) methyl ether methacrylate), and lauryl methacrylate, which provide the final product with tunable reactivity and balance between hydrophilicity and hydrophobicity. The detailed study of the copolymer synthesis and properties has been carried out to establish the most efficient pathway to design and tailor this amphiphilic molecular brush system for specific applications. As an example of the applications, we showed the ability to control the deposition of graphene oxide (GO) sheets on both hydrophilic and hydrophobic surfaces using GO modified with the molecular brushes. Also, the capability to tune the osteoblast cell adhesion with the copolymer-based coatings was demonstrated.

KEYWORDS: surface modification, molecular brushes, functional coatings, graphene modification, biomedical applications

■ INTRODUCTION

The modification of surfaces and colloidal structures allows for the fine-tuning of their properties, which becomes crucially important for design and compatibilization of components within complex functional systems. 1,2 The natural variability of substrates and diversity of the desired properties call for methods of surface modification that could deliver required characteristics to a wide range of materials in a most straightforward and cost-effective way. To this end, grafted polymer layers have drawn considerable attention because of their ability to control surface properties of modified substrates, robustness of the layers, and diversity of chemistries suitable for the layer formation. ¹⁻¹¹ Despite the fact that significant advancements in synthesis of the grafted polymer layers have been made over the recent years, the developed protocols of interface modifications face challenges when being implemented in a large-scale manufacturing setup. Indeed, typical grafting procedures are multistep processes where every stage inevitably imposes limitations on the nature of the substrate, generates solvent/chemical waste, and complicates the overall operation. Thus, there is a demand for environmentally-friendly surface modification protocols with a minimum number of technological steps. To this end, we have demonstrated that functional grafted polymer layers, in principle, can be obtained in a single step (from water or with minimal use of solvents and without postprocessing rinsing) using reactive (brushlike) copolymers.

Specifically, the present article focuses on cross-linkable amphiphilic (statistical) copolymers (Scheme 1) containing oligo(ethylene glycol) methyl ether methacrylate (OEGMA), glycidyl methacrylate (GMA), and lauryl methacrylate (LMA), which can be straightforwardly covalently attached to a number of solid surfaces and colloidal objects. Most of the copolymers synthesized in this work represent a class of macromolecules called molecular (or bottle) brushes, which have a long polymer backbone with relatively long densely packed side chains. 1 The selection of monomers for making molecular brushes with tailored affinity is based on their complementary functionality. Poly(oligo(ethylene glycol) methyl ether methacrylate) (PO-EGMA) has drawn significant attention over the recent years

Received: December 29, 2017 Accepted: April 2, 2018 Published: April 2, 2018

[†]Department of Materials Science and Engineering and [‡]Department of Bioengineering, Clemson University, Clemson, South Carolina 29634, United States

[§]Department of Orthopaedics, Medical University of South Carolina, Charleston, South Carolina 29425, United States

Nanostructured Materials Laboratory, University of Georgia, Athens, Georgia 30602, United States

^LSchool of Materials Science and Engineering, Georgia Institute of Technology, Atlanta, Georgia 30332, United States

ACS Applied Materials & Interfaces

Scheme 1. Chemical Structure of Statistical Copolymers Synthesized in This Work from the Following Monomers: GMA, LMA, and OEGMA, and General Schematic of the Brushlike Copolymer: N_{SC} is a degree of polymerization of OEGMA or LMA side chains and N_G is the degree of polymerization of the backbone spacer between OEGMA or/and LMA side chains

because of its thermosensitivity, protein repellency, and ability to compatibilize materials with water. $^{10,16-22}$ Indeed, OEGMA monomers bearing a reactive methacrylate fragment are capable of undergoing polymerization while a quite long oligo(ethylene glycol) side moiety provides water compatibility to the synthesized macromolecule. The balance between hydrophilic and hydrophobic parts of the molecule results in thermal switching properties that strongly depend on the side-chain length. 21 It is well-established that poly(ethylene glycol) (PEG) demonstrates low cellular toxicity and does not trigger immune system response, which facilitates the use of POEGMA for biological and biomedical applications. 16-22 Poly(glycidyl methacrylate) (PGMA), which is insoluble in water, has been applied for the efficient modification of various surfaces using a "grafting-to" method. 9,23-28 This method involves reaction of functionalized polymers with complimentary functional groups located on the substrate surface. GMA can be easily copolymerized with various monomers through solution freeradical copolymerization. Most importantly, epoxy groups of GMA can react with nucleophilic groups (such as hydroxyl, carboxyl, and amino), which opens wide opportunities for postsynthesis modifications.^{9,29–31} As the opening of an epoxy group generates a hydroxyl group, PGMA can be thermally cross-linked, forming a stable permanent network layer. 24,28,32 LMA has been employed as a hydrophobic/lyophilic and low- $T_{\rm g}/{\rm crystallizable}$ component in a number of studies 33-35 and was selected in the present study to tune the hydrophilic/ hydrophobic balance of the resulting molecular brushes. Thus, in our chemical design, it is possible to combine various practically important functionalities within a single complex architecture of the copolymer molecular brush. Recently, we have demonstrated that surface modification with GMA-

OEGMA-based molecular brushes can be used to dramatically enhance the thermal stability of the enzymes so they can maintain their catalytic activity after being subjected to temperatures over 100 °C. 36 Also, the GMA-OEGMA copolymer allows formation of a highly conductive and transparent reduced graphene oxide (rGO) bilayer film.³⁷

In this work, the copolymers have been synthesized by conventional free-radical polymerization. To this end, we have performed a detailed investigation of the copolymerization of GMA, OEGMA, and LMA. We have identified reactivity ratios in this system, which are necessary for the control of the copolymer composition. We also performed analysis of the macromolecular architecture of the copolymers obtained and determined that majority of the materials have the characteristics of molecular (or bottle) brushes. The thermal properties, surface energy, and water solubility of the series of copolymers have been characterized. We demonstrated that these materials can be straightforwardly anchored (using the grafting-to method) to macroscopic surfaces or colloidal objects from melt and solution to form functional coatings. Specifically, it was shown that accurate control over cell adhesion and growth can be achieved using grafted layers made of PGMA, P(GMA-LMA), P(GMA-OEGMA), and P(GMA-OEGMA-LMA) macromolecules. We have also performed grafting modification of graphene oxide (GO) sheets with P(GMA-OEGMA) and P(GMA-OEGMA-LMA) molecular brushes. The modification allowed for the deposition of nearly perfect GO monolayers on either hydrophilic or hydrophobic surfaces by dip-coating from water. These examples are clear evidence that the molecular brushes reported here can be readily used for one-step surface modification of objects of different nature. In general, our results indicate that the use of the highly branched reactive macromolecules in grafting modification allows anchoring a significant number of functional moieties (epoxy, PEG, and/or lauryl in this work) via straightforward one-step grafting-to attachment. It is also necessary to highlight that, to the best of our knowledge, this article present the first example of covalent anchoring of molecular brushes to surfaces via the grafting-to approach using multiple reactive (epoxy) groups located along the polymer chain.

■ EXPERIMENTAL SECTION

Materials. GMA (97%), azoisobutyronitrile (AIBN), OEGMA [average M_n 950, containing 100 ppm monomethyl ether hydroquinone (MEHQ) and 300 ppm BHT as the inhibitor], LMA, and inhibitor removers [replacement packing for removing hydroquinone and MEHQ and replacement packing for removing tert-butylcatechol] were purchased from Sigma-Aldrich. All solvents used in this study were purchased from VWR International and used as received. Alpha minimum essential medium (α MEM), fetal bovine serum (FBS), penicillin, and streptomycin were purchased from Corning Inc. (Manassas, VA). Cell line (7F2) was purchased from ATCC (Manassas, VA). Ethanol (200 proof) was obtained from Sigma-Aldrich (St. Louis, MO). Osmium tetroxide and hexamethyldisilazane were acquired from Electron Microscopy Sciences (Hatfield, PA). A LIVE/DEAD Viability/Cytotoxicity kit was purchased from Thermo Fisher Scientific (Waltham, MA).

Synthesis of the Binary Copolymers. MEHQ inhibitor remover beads were added to GMA and LMA prior to synthesis. MEHQ and BHT inhibitor remover beads were added to OEGMA dissolved in methyl ethyl ketone (MEK) prior to synthesis. Solutions were then filtered through the 0.2 μ m syringe poly(tetrafluoroethylene) filters. The resulting monomers as well as pure solvent and AIBN solution were purged under nitrogen for 45 min and then added in proper amounts to vials in a nitrogen-purged glovebox. These vials were

sealed with a septum and then immersed into a water bath preheated to 50 °C. The overall molar monomer concentration was 0.5 mol L^{-1} and the AIBN concentration was 0.01 mol L-1. GMA-OEGMA synthesis was terminated after 1.5 h, OEGMA-LMA after 2 h, and GMA-LMA after 5 h. The resulting copolymers were precipitated by diethyl ether addition, centrifuged, and redissolved in MEK. This procedure was repeated three times to remove unreacted monomers and initiator. To reduce the polydispersity in the copolymer composition (connected to the reactivity ratios for monomer pairs) and molecular weight of the polymers, we stopped the polymerizations at low (10-15%) values of the monomer conversion.

Synthesis of the Terpolymers and Homopolymers. Homopolymers (PGMA and POEGMA) and copolymers were synthesized by solution free-radical polymerization. Monomers were prepared using the same technique as during the study of binary systems. The charged LMA-OEGMA-GMA molar ratios were 0:0:100, 0:100:0, 0:80:20, 12.5:75:12.5, and 20:60:20. The overall monomer concentration was 0.5 mol L⁻¹, and the AIBN concentration was 0.01 mol L⁻¹. The solution was kept under nitrogen purge for 45 min and then immersed into a water bath preheated to 50 °C. The polymerization reaction was terminated after 1.5 h by opening the flask to the ambient atmosphere and removing the reactor from the water bath. The product of the reaction was purified using the same technique as for the study of the binary systems. To prepare P(GMA-OEGMA) copolymer with lower molecular weight, carbon tetrabromide (0.02 mol L-1) was added to the reaction mixture. To reduce the polydispersity in the copolymer composition (connected to the reactivity ratios for monomer pairs) and molecular weight of the polymers, we stopped the polymerizations at low (10-15%) values of the monomer conversion.

Analysis of the Copolymer Composition. Nuclear magnetic resonance (¹H NMR) analysis was done using a Bruker AVANCE-300 spectrometer and TopSpin 1.3 PL4 software and processed with Delta 5.0.4 software. The copolymer composition was also investigated by attenuated total reflectance Fourier transform infrared (ATR-FTIR) spectroscopy. A Thermo Nicolet Magna 550 FTIR spectrometer with the Thermo-Spectra Tech Endurance Foundation Series Diamond ATR accessory was used, and 16 scans were averaged. An ATR correction and baseline correction were performed using Thermo Scientific OMNIC software version 8.0. Data processing and plotting were completed using Origin MicroCal 9.

Analysis of the Copolymer Thermal Properties. Differential scanning calorimetry (DSC) (model 2920; TA Instruments) was carried out at a heating/cooling rate of 20 °C/min. The temperature range of the experiment was set from -100 to 100 °C. The samples were heated, cooled, and the reheated again. The second heating was used to measure the glass-transition temperature and meting point. The glass transition is reported as the inflection point on the heat flow graph.

Analysis of the Copolymer Molecular Weight and Water Compatibility. Dynamic light scattering (DLS) has been used to estimate the molecular weight of the synthesized polymers. We could not use standard size exclusion chromatography because of the high molecular weight of the polymers obtained. Namely, Malvern Zetasizer ZS DLS and zeta potential (DLS-Zeta) instrument was utilized to characterize the size of polymer coil in water and MEK. To estimate the molecular weight, a set of monodisperse polystyrene standards with molecular weights ranging from 200 up to 3000 kDa dissolved in MEK was used for the calibration. The resulting data were fitted with a linear function in MW^{0.5}-size coordinates. It was further recalculated into the molecular weight using NMR data regarding copolymer composition. Atomic force microscopy (AFM) was performed to determine fully extended length for selected macromolecules using Bruker multimode 8 in the tapping mode. The AFM probes with a tip radius of ~2 nm (ScanAsyst-air) were employed. Copolymer samples were deposited by spin-coating (at 2000 rpm) from 0.1 mg mL⁻¹ water solution on the mica surface. The solution concentration was adjusted to obtain the monolayer of individual chains deposited on the surface and avoid crossing of the macromolecules. The AFM

micrographs were further processed using the grain analysis module in the Gwyddion modular program.

Grafting of Copolymers to a Silicon Wafer Surface. The polymer layers were deposited and grafted according to a previously published procedure.²⁴ In brief, highly polished, single-crystal undoped silicon wafers (University Wafer: (100), 10 000-20 000 Ω·cm, 500 μ m) were used as a substrate. The wafers were cleaned in "piranha" solution (3:1 concentrated sulfuric acid/30% hydrogen peroxide) for 4 h and then rinsed several times with deionized (DI) water. After rinsing, the substrates were dried under a stream of dry nitrogen. Copolymers were deposited on the surface of the clean dry wafers by dip-coating (Mayer Feintechnik dip coater, model D-3400) from the MEK solution. After evaporation of MEK, the samples were placed on the temperature gradient stage, 24 with the temperature varying along the stage surface for different times. After the grafting, the samples were removed from the stage and thoroughly washed to remove any ungrafted copolymer. For the removal, the samples were placed in a vial filled with MEK and placed on an orbital shaker for 15 min and then the MEK was changed. After five cycles of washing and solvent removal, the film thickness was investigated using a custom-built scanning spectroscopic reflectometer.²⁴ In preceding studies, we determined that this rinsing procedure is sufficient to remove all ungrafted polymer. A total of 114 points on a 6×19 mm scan with 1 mm resolution were measured with a 10 ms acquisition time per point. The thicknesses at the points were averaged for each copolymer film and then subsequently plotted with Origin 9.0 software. Analysis of water and hexadecane contact angles (HCAs) was done using a KRUSS DSA10 drop shape analyzer at 20 s after droplet deposition on the grafted copolymer surface.

Preparation of GO Sheets Modified with Copolymers. The GO aqueous suspension was prepared by the Hummers' method.³⁸ Natural 300-mesh graphite powders (Alfa Aesar) were added with sodium nitrate (2.5 g) in sulfuric acid (98%, 107 mL), which was cooled to 0 °C before mixing. Then, potassium permanganate (15 g) was slowly added with vigorous stirring to avoid the temperature rising above 20 °C. The mixture was heated to 35 \pm 3 °C and maintained for 30 min before adding water (214 mL), waiting for the temperature to rise to 98 °C and maintaining for 15 min. Finally, warm water (850 mL) and hydrogen peroxide (30%, 1-2 mL) were added sequentially to dissolve the side products of the oxidation (black particulates), during which the color of the solution turned from dark brown to bright yellow. The as-synthesized GO suspension was purified by water rinsing and ultracentrifugation (10 000 rpm for 1 h) five times to remove the electrolytes and protons. GO water suspension (~3 mg mL^{-1}) was mixed with water solution of copolymers (\sim 5 mg mL⁻¹) in a mass ratio of 1:6, so as to have polymer in excess. The mixture was rigorously shaken for 15 min and then maintained at room temperature (RT) on an orbital shaker. After a minimum of 4 h, the GO sheets were evacuated from the solution by centrifugation at 10 000 rpm for 5 min and rinsed 3-4 times with DI water to remove unattached polymer chains. This suspension was then centrifuged at 1000 and 500 rpm for 15 min at least twice to remove all flocculated sheets

Formation of the GO/Copolymer Monolayers. The undoped silicon wafers were used as a substrate. Before deposition of the GO/ copolymer monolayer, the wafers were first cleaned in an ultrasonic bath for 30 min, placed in a hot piranha solution for 1 h, and then rinsed several times with high purity DI water. After being rinsed, the substrates were dried under the stream of nitrogen (purchased from Airgas) in cleanroom 100 conditions. The surface of the clean silicon wafer became completely hydrophilic, which was confirmed by ~zerodegree water contact angle (WCA). Self-assembled monolayers on silicon substrates were fabricated to study the deposition of the GO on the hydrophobic surface. 39 For this, we vapor-deposited 0.9 nm chlorodimethyl-n-octylsilane (97%, purchased from Alfa Aesar) on hydrophilic Si substrates overnight. Then, these substrates were rinsed in MEK three times for 10 min each time and then for 2 h. Next, the silane-modified substrates (with a WCA ranging from 90° to 100°) as well as the hydrophilic substrates (with a WCA effectively equal to 0°) were dip-coated from the GO/copolymer dispersion. The dip-coating

Table 1. Composition and Type of the Copolymers Synthesized (Scheme 1)

copolymer	OEGMA fraction		LMA fraction		GMA fraction		
	molar	weight	molar	weight	molar	weight	copolymer type
			P(GMA-0	DEGMA)			
$P(G_{85}-O_{15})$	0.15	0.54			0.85	0.46	LM
$P(G_{73}-O_{27})$	0.27	0.71			0.73	0.29	DM
$P(G_{61}-O_{39})$	0.39	0.81			0.61	0.19	DM
$P(G_{34}-O_{66})$	0.66	0.93			0.34	0.07	DM
			P(GMA	-LMA)			
$P(G_{83}-L_{17})$			0.17	0.27	0.83	0.73	DC/LM
$P(G_{65}-L_{35})$			0.35	0.49	0.65	0.51	DM
$P(G_{46}-L_{54})$			0.54	0.68	0.46	0.32	DM
$P(G_{26}-L_{74})$			0.74	0.84	0.26	0.16	DM
			P(GMA-OE	GMA-LMA)			
$P(G_{15}-O_{66}-L_{19})$	0.66	0.90	0.19	0.07	0.15	0.03	DM^a
P(G ₂₈ -O ₅₆ -L ₁₆)	0.56	0.87	0.16	0.01	0.28	0.06	DM^a

^aOnly OEGMA monomeric units were considered in calculations.

was conducted from a 0.025 wt % GO water suspension at a 300 mm/ min withdrawal speed. Morphology, microstructure, and changes in thickness of individual GO sheet after modification with the polymers were studied with a Dimension 3100 (Veeco Digital Instruments, Inc.) in the tapping mode. Silicon tips with a spring constant of 50 N m⁻¹ were used for all scans at 1 Hz. Analysis of AFM images was carried out using Gwyddion (version 2.45) software. To reveal the thermal decomposition behavior of GO before and after modification with the copolymer, thermogravimetric analysis (TGA) was performed using a Q-5000 TA Instruments and AutoTGA 2950HR V5.4A under a N2 environment from RT to 600 °C using a ramp rate of 15 °C/min. To study the adsorption kinetics, we mixed 3 mg mL⁻¹ concentrated water solution of adsorbent (GO) with 5 mg mL⁻¹ copolymer solution in water in a ratio of 1:6. Such a system was held at RT. Then, we gently evacuated a small amount of the suspension after 20, 60, 150, and 270 min of adsorption and rinsed it well with DI water at least

In Vitro Evaluation of Cell Adhesion. Polished silicon wafers prepared as specified above were coated with polymer solutions in MEK via dip-coating and annealed for 4 h at 130 °C [PGMA and P(GMA-LMA)] or at 80 °C [P(GMA-OEGMA) and P(GMA-OEGMA-LMA)]. The resulting films were washed in pure MEK to remove the ungrafted polymer. Prior to the experiments, 7F2 cell line was cultured in α MEM supplemented with 10% of FBS and 1% of penicillin and streptomycin. Cells were incubated at 37 °C in 5% CO₂. Upon reaching 80% confluency, osteoblasts were passaged, diluted to a concentration of 10⁵ cells/mL, and transferred into a sterile 24-well plate containing studied samples. Then, the samples were incubated for 2 days at 37 °C in 5% CO₂. The growing medium was replaced every 24 h. Following the incubation, the samples were visualized by means of scanning electron microscopy (SEM) (SEM Hitachi S4800). To prepare the samples for SEM, the following methodology was used. The samples were exposed to 2.5% glutaraldehyde for 2.5 h at RT. Afterward, the additional postfixation was implemented by submerging the samples in 1% osmium tetroxide solution for 2.5 h at RT. Following the dehydration in ethanol gradient (50, 75, 90, and 100%), the samples were rinsed twice in 100% hexamethyldisilazane. SEM visualization was performed using an acceleration voltage of 5 kV and a working distance of 6 mm. In addition, the viability of osteoblasts attached to the samples was assessed by the LIVE/DEAD assay according to the protocol described elsewhere. Briefly, upon osteoblast attachment, the samples were rinsed with 5 mL of sterile phosphatebuffered saline and exposed to calcein AM (20 μ M) with ethidium homodimer-1 (4 μ M) for 30 min at RT. Then, the samples were visualized by means of fluorescent microscopy (Thermo Fisher EVOS FL Auto).

RESULTS AND DISCUSSION

Synthesis and Parameters of Copolymers. GMA provides the copolymers with the ability to bind with the surfaces and cross-link in a one-step procedure, whereas OEGMA and LMA deliver compatibility of the modified object with hydrophilic and hydrophobic surfaces/media, respectively. Through composition, the properties of the copolymers can be finely tuned for a specific application. To obtain precise control over this process, it was necessary to identify the reactivity ratios for the monomers participating in the copolymerization reaction. It is well-established that the monomer compositions in the feed and in the synthesized polymer are generally different because of the different abilities of the monomers to attach to a growing polymer chain. 40 Classical Mayo-Lewis equation (see Supporting Information: S1) considers this effect, and the process of (free-radical) copolymerization generally can be described in terms of reactivity ratios r_{12} and r_{21} . To establish the ratios of the composition of the synthesized copolymers, they were investigated with NMR and further analyzed with Fineman-Ross, inverted Fineman-Ross, and Kelen-Tüdos plots (Supporting Information: S1, Figure S1). These methods are commonly used to extract the reactivity ratios from the experimental data sets. 41 In brief, the composition of the copolymers is plotted against the monomer ratio in the feed in a certain system of coordinates, which is different for each method. The linearization of these data allows for the calculation of the reactivity ratios, which should be reasonably close for all three methods. For all of the systems studied here, linear function fits the experimental data quite well, which points out that the formalism of reactivity ratios is applicable here and the use of nonlinear fitting is not required. To complement NMR results (Supporting Information: S1), additional analysis of the copolymer composition has been performed using FTIR spectroscopy (Supporting Information: Figure S2 and Table S3). In general, FTIR data coincide with the NMR results. The composition of the copolymers synthesized in this work is listed in Table 1. For the sake of conciseness, we shortened the abbreviated titles of the copolymers having certain compositions and used only the first character of the monomer name.

To determine molecular parameters for the brushlike polymers, we followed the definitions and phase diagrams outlined in the recently published manuscripts. 14,15 In general, the brushlike macromolecules can be divided into four major classes: (a) loosely grafted combs (LC), (b) densely grafted combs (DC), (c) loosely grafted molecular (bottle) brushes (LM), and (d) densely grafted molecular (bottle) brushes (DM). The major structural parameters involved in the differentiation between the classes are (Scheme 1) (i) the degree of polymerization of side chains, N_{SC} , and (ii) the degree of polymerization of the backbone spacer, N_G . We conducted detailed structural analysis of the copolymers based on their chemical composition (Supporting Information: S3, Table S2), and it was determined that majority of the macromolecules obtained in this work can be classified as densely grafted molecular brushes (Table 1).

The reactivity ratios for the GMA-OEGMA system were estimated to be $r_{\rm GMA}=1.4$ and $r_{\rm OEGMA}=0.3$, respectively, for GMA-LMA $r_{\rm GMA}=1.2$ and $r_{\rm LMA}=0.7$ and for LMA/OEGMA $r_{\rm LMA}=0.6$ and $r_{\rm OEGMA}=0.4$. The values obtained here clearly reveal the suppressed reactivity of the methacrylate macromonomers (OEGMA and LMA) as compared to the reactivity of GMA. We associate this phenomenon with the hindered diffusion of the monomer double bounds to the radical at the end of the growing polymer chain. In fact, the reactivity ratio indicates the tendency of the growing polymer chain to react preferentially with a certain type of monomer. The r_{GMA} value above 1 indicates the tendency of the growing chain with a GMA unit at the end to react with GMA, whereas r values below 1 point out an opposite trend, where chains with OEGMA-LMA monomeric units at the end have a tendency to react with a dissimilar monomeric unit. All three monomers used here belong to the methacrylate family, which implies that the stabilization of the monomer radical is almost the same. However, their diffusion properties and steric hindrance effects are significantly different because of the difference in the molecular weight. This leads to GMA being the most active monomer in these systems, whereas LMA and especially OEGMA show suppressed reactivity during the copolymerization. This effect has been previously demonstrated for macromonomer copolymerization and specifically for OEGMA copolymerization with 2-vinylpyridine. 41 We note that in that study, OEGMA (300 g/mol) has been shown to be more reactive than OEGMA (1100 g/mol), highlighting the influence of molecular weight on the reactivity of the polymer. Using the reactivity ratios, we predicted the terpolymer compositions using copolymerization equations published elsewhere. 40 The calculated compositions quite closely matched the experimentally measured ones (Supporting Information: S2, Table S1). The observed deviation lies within 5% and is typical for the calculations involving reactivity ratios. It is evident that our detailed analysis of the copolymerization between GMA, LMA, and OEGMA monomers allows for the controlled synthesis of the copolymers with a particular composition.

From the values of reactivity ratios, general microstructure of the copolymers can be outlined.⁴⁰ First of all, the values indicate that the copolymers being obtained are not random because the product of reactivity ratios is not equal to 1. Also, the macromolecules synthesized do not have a block copolymer structure because at least one of the reactivity ratios for the monomer pairs has a value below one. The polymers represent the case of statistical copolymers in which sequential distribution of the monomeric units obeys known statistical laws. In the statistical copolymers, the microstructure is defined by the sequence length distribution, which is distribution of the

various lengths of the monomer 1 and monomer 2 sequences. Using known statistical relationships, 40 we estimated the distribution for P(G₃₄-O₆₆) and P(G₂₆-L₇₄) copolymers (Supporting Information: Figures S10 and S11) and found that the macromolecules do not have significant fractions of long microblocks of more active monomer (GMA) or majority monomer (OEGMA and/or LMA).

DLS was employed to estimate the copolymer degree of polymerization with subsequent calculation of the molecular weight (Supporting Information: S5, Figure S3). In our measurements for calibration, we used polystyrene standards. We found that the degree of polymerization tends to increase when the OEGMA or LMA molar ratios are increased, reflecting the progressive suppression of the termination step by steric hindrance caused by the macromonomers. 42 The typical values of degrees of polymerization are in the range of 2000-8000; however, as LMA and especially OEGMA have relatively high molecular weights, the molecular weight for the copolymer ranges from 10⁵ to 10⁷ g/mol (or Da).

AFM revealed (Figure 1a) that copolymers [as exemplified by P(G₃₄-O₆₆)] have a linear structure, and beside randomly

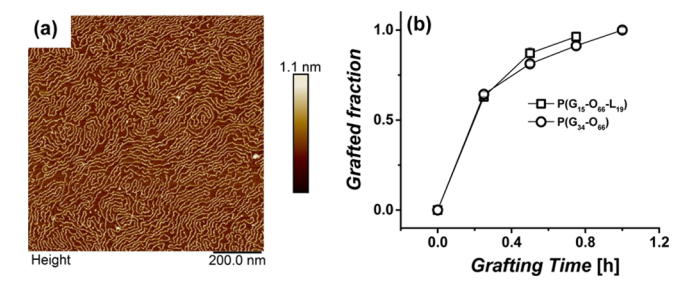


Figure 1. (a) AFM topographical image of the P(G₆₆-O₃₄) copolymer solvent casted on a mica surface. (b) Grafted fraction (thickness of the grafted film/thickness of the deposited film) vs grafting time dependence for P(G₆₆-O₃₄) and P(G₁₅-O₆₆-L₁₉). The thickness of the initially deposited copolymer film was approximately 150 nm. The temperature of the grafting was 80 °C.

distributed side chains, no branching is observed. We analyzed 75 macromolecules and found that the average length of this molecular brush is equal to 497 ± 216 nm. The fully extended length L of the polymer molecule can be approximated mathematically as follows: 43,44

$$L = 2N_{\rm n}d\,\sin\!\left(\frac{109.5}{2}\right) \tag{1}$$

where N_n is the number average degree of polymerization, d is the length of the carbon-carbon bond (0.154 nm), and 109.5° is the angle between two bonds in the case of an sp³-hybridized carbon atom. The number- and weight-average degrees of polymerization are 1976 and 2677, respectively. The numberand weight-average molecular masses are found to $M_{\rm n} = 1334$ kg/mol and $M_{\rm w}$ = 1807 kg/mol, respectively, which yield a polydispersity index of 1.36. We used the AFM data to estimate the root-mean-square values of end-to-end distance $\langle R^2 \rangle^{1/2}$ and radius of gyration $(\langle R_{\rm g}^{\ 2} \rangle^{1/2})$ for the methacrylic copolymer coil in theta solvent/bulk. The values for the copolymer (Gaussian) chain are given by the following relationships: 14,44

$$\langle R^2 \rangle^{1/2} = (blN)^{1/2} \tag{2}$$

$$\langle R_{\rm g}^2 \rangle^{1/2} = \langle R^2 \rangle^{1/2} / \sqrt{6} \tag{3}$$

where b is the Kuhn segment, l is the monomeric length, and Nis the degree of polymerization. Because the backbone of the graft copolymer is made from methacrylic monomers, as a first approximation, we used in our estimations the parameters known for methyl methacrylate (Supporting Information: S3). N determined experimentally from the DLS experiments is close to the weight-average value; 45 therefore, we used weightaverage N in the calculations. It was found that $\langle R^2 \rangle^{1/2}$ and $\langle R_{\rm g}^2 \rangle^{1/2}$ are equal to 29 and 12 nm, respectively. The values of degree of polymerization, molecular weight, and size of the polymer coil determined from AFM are in quite good agreement with the values of degree of polymerization (~3000), molecular weight (~2000 kg/mol), and hydrodynamic diameter [\sim 26.5 nm in MEK] of P(G_{34} - O_{66}) obtained from the DLS measurements, respectively.

It is necessary to point that the end-to-end distance and radius of gyration of the P(G₃₄-O₆₆) macromolecules deposited on the mica surface from water (2D chain conformations, Figure 1a) were found to be 225 \pm 123 nm and 88 \pm 40 nm, respectively. This experimental fact indicates that the copolymer chains strongly interact with the mica surface and spread well above their DLS hydrodynamic diameter in water (\sim 60 nm). However, the ratio of those values was found to be 2.56, which is very close to $\sqrt{6}$ = 2.45, which can be predicted for Gaussian coil.

Thermal Characteristics of the Copolymers. Thermal properties of polymers, such as glass-transition (T_{σ}) and meting temperatures (T_m), significantly affect the parameters for the polymer grafting because polymer solubility and diffusion are involved in the anchoring process. To this end, we have performed DSC studies for the synthesized copolymers (Supporting Information: Figure S4). It is well-established that the thermal properties of statistical copolymers are related to the thermal properties of homopolymers made of the monomers constituting the copolymers.⁴⁶ The properties of the homopolymers are as follows. PGMA does not exhibit any crystallinity, while glass-transition temperature is found to be ~75 °C. Poly (lauryl methacrylate) (PLMA) is a semicrystalline polymer⁴⁷ with $T_{\rm m}$ at \sim -26 °C and $T_{\rm g}$ at \sim -50 °C.⁴⁸ To determine the thermal characteristics for the OEGMA homopolymer, we obtained POEGMA using the same radical polymerization procedure as was used to synthesize the copolymers. DSC indicated that POEGMA is a semicrystalline polymer with $T_{\rm g} \approx -60~{\rm ^{\circ}C}$ and $T_{\rm m} \approx 26~{\rm ^{\circ}C}$. It is necessary to point that crystallinity for the atactic PLMA and POEGMA originates from crystallization of the high-molecular-weight side groups. Therefore, the copolymers can retain this side-group crystallization, or the crystallization observed for the homopolymers can disappear as a result of the copolymerization. T_{σ} values for the statistical copolymers have to be somewhat between T_g of PLMA/POEGMA and T_g of PGMA and related to weight fractions of the monomeric units in the copolymers.⁴⁶

The analysis of DSC curves is shown in Figure S4 (Supporting Information). There is no crystallinity observed for P(GMA-LMA) copolymers. The glass transition for the copolymers is observed to gradually decrease from 55 to -10°C with increasing LMA content from 0.15 to 0.74 molar fraction (from 0.27 to 0.84 weight fraction) (Figure S4a). We also observed LMA side-chain-related thermal transition when the LMA mole fraction is equal to 0.54 and 0.74 (0.68 and 0.84 weight fraction) at about -60 °C. This transition is, to a certain extent, below $T_{\rm g}$ for the LMA homopolymer. We associate this transition with the onset of lauryl side-chain movement. On the

contrary, P(GMA-OEGMA) copolymers demonstrate crystallinity originating from the side groups when the OEGMA molar fraction is above 0.15 (0.54 weight fraction) (Supporting Information: Figure S4b) with $T_{\rm m}$ approximately the same as the one for POEGMA. P(GMA-OEGMA) copolymers have T_{σ} between -40 and -60 °C. T_g is dominated by OEGMA because of the high monomer weight fraction. The transitions for the terpolymer P(G₁₅-O₆₆-L₁₉) synthesized here possess thermal properties, which are close to the properties of the P(GMA-OEGMA) copolymers with a glass-transition temperature at \sim -31 °C and a melting temperature at \sim 32 °C. The properties of the terpolymer are dominated by OEGMA because of the high weight fraction (0.9) of the monomeric unit in the macromolecule. It is obvious that the surface modification by the melt grafting-to method has to be conducted above T_g for the P(GMA-LMA) copolymers and above $T_{\rm m}$ for the OEGMA-containing copolymers.

Grafting from the Melt. In our work, we have used the grafting-to approach for surface modification using the copolymers synthesized.9 This method involves reaction of functionalized polymers with complimentary functional groups located on the substrate surface. The major advantage of the grafting-to technique over other methods is that the polymer chains can be carefully characterized prior to attachment, resulting in well-defined grafted layers. Furthermore, the grafting-to technique is often less challenging from a chemical standpoint because it does not involve elaborate synthetic protocols. In this method, processes of synthesis and modification are separated in space and time; thus, the conditions of the synthesis are no longer restrained by the substrate and chemical proficiency of the operator. In our design, the surface modification with the copolymers is a straightforward process, where the copolymer, dissolved in water or solvent, is deposited as a film on a surface by dipcoating, spin-coating, spray-coating, or drop-casting. The copolymer concentration and processing parameters dictate the film thickness. The resulting layer then is anchored to the surface and cross-linked by annealing to ensure the effective surface binding and stability in liquid media. The kinetics of this process is a key component enabling the synthesis where all deposited polymer is grafted and cross-linked, and therefore, the grafted film does not require post-treatment with solvents to extract the unbounded polymer.

GMA contains the reactive epoxy groups that allow for surface binding through reactions with nucleophilic groups on the substrate of the modification. Such chemical groups as amino, carboxyl, and hydroxyl groups, which are commonly found on the various surfaces, can promote the opening of the GMA epoxy rings. In case when the surface lacks the required groups, the plasma treatment of the surface can be conducted to initiate the binding with the polymer.⁴⁹ Once the GMA has reacted with the surface, it can further undergo cross-linking through the following mechanism: the opening of an oxirane ring creates newly formed hydroxyl groups that can further react with the neighboring epoxy groups. Thus, the process of GMA-based copolymer surface modification is essentially the same for a variety of objects and can be easily transferred between different types of substrates.9 The formation of a nonsoluble covalently attached layer proceeds from the surface and propagates into the polymer bulk. Because this process is temperature-dependent (similarly to the curing of the epoxy resin), the duration of the surface modification and the temperature of this process are two primary parameters influencing the resulting thickness of the coating.

Figure 1b displays the kinetics of the Si wafer modification with molecular brushes P(G₃₄-O₆₆) and P(G₁₅-O₆₆-L₁₉) conducted at 80 °C. The thickness of the layer deposited initially on the wafer by dip-coating is ~150 nm. It is evident that upon fast reaction with the hydroxyl groups located on the surface and formation of the initial 100 nm thick cross-linked layer, the reaction proceeds further in a decelerating fashion. However, by selecting proper conditions for annealing, it is possible to fully graft/cross-link films of several hundred nanometers in thickness. In general, from multiple grafting experiments using a combinatorial approach (employing a temperature gradient stage), 9,24 we made an empirical conclusion that there is a certain threshold grafting temperature above which all polymer deposited on the surface is grafted. Below this temperature, it is impossible to obtain a grafted film nonextractable by the solvent polymer, even if the grafting is conducted for several days. For the PGMA homopolymer used in this work, it is \sim 90 °C. There is also a threshold time that is needed at the threshold temperature to reach the complete grafting/cross-linking for the submicron grafted films. If the duration of the copolymer anchoring is shorter than the threshold time, there is unattached (extractable with solvent) polymer in the grafted layer. For PGMA, the threshold time at 90 °C is about 2 h. Addition of LMA increases this temperature by 35° to about 120–125 °C (Figure 2a). The threshold time is

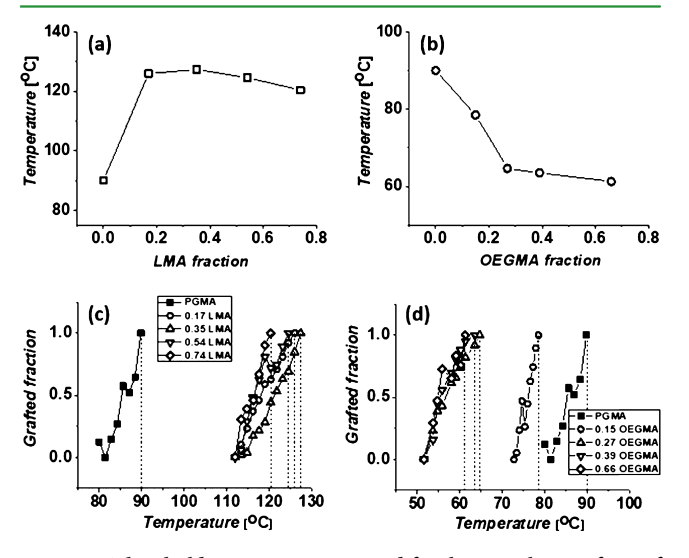


Figure 2. Threshold temperature required for the complete grafting of a submicron layer made of P(GMA-LMA) (a) and P(GMA-OEGMA) (b) as a function of the molar copolymer composition. Grafted fraction (thickness of the grafted film/thickness of the deposited film) as a function of the grafting temperature for P(GMA-LMA) (c) and P(GMA-OEGMA) (d). Grafting time: (a,c) 4 h and (b,d) 16 h. In the legend for the figures (c,d), molar fractions of LMA/OEGMA are indicated. For PGMA, the grafting time is 4 h (c,d).

also increased to about 4 h for the GMA–LMA copolymers. An entirely different dependence is observed for the GMA–OEGMA copolymers, where with the OEGMA addition, the threshold time is increased to 10–16 h. At the same time, the threshold temperature is significantly (10–30 °C) decreased when OEGMA is incorporated into the copolymer chain (Figure 2b). We found that the process of the (complete) grafting/cross-linking can be well-controlled. For instance,

Figure 2c,d illustrates how the variation of the grafting temperature at a constant time influences the thickness of the grafted layer. Indeed, grafting of P(GMA-OEGMA) and P(GMA-LMA) binary copolymers is strongly promoted as the temperature increases. However, because the grafting of the submicron films depends on multiple parameters (e.g., concentration and spatial distribution of GMA units in the copolymer; diffusion rate of the macromolecules, chain segments and side groups; and rate and extend of the reaction between substrate surface and GMA groups), we cannot offer at this time comprehensive description of the observed dependencies. However, we identified an effective combinatorial methodology to determine the threshold temperature and time for the copolymers. It is necessary to point that the grafting of GMA-based copolymers involves only a small fraction (~10%) of epoxy groups, which implies that the grafted layers can be further modified using unreacted epoxy functionalities (Supporting Information: S12).

Surface Energy and Wettability. In our next step, we determined the wettability and surface energy for the grafted copolymer films with the submicron thickness on the level of 200–800 nm. The WCA and HCA were measured. It turns out that hexadecane virtually completely wets all studied copolymer and PGMA films, yielding an extremely low contact angle. The WCA for the PGMA homopolymer film was found to be about 75°. As it can be anticipated, the WCA is systematically increasing with LMA fraction (Figure 3a) and decreasing with

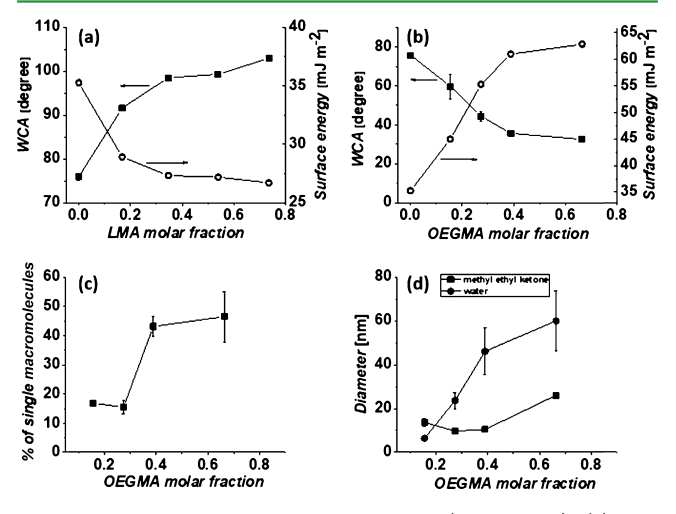


Figure 3. WCAs and surface energies of P(GMA-LMA) (a) and P(GMA-OEGMA) copolymers (b) grafted from melt coatings. Results of DLS measurements for P(GMA-OEGMA): % of single macromolecule signal in DLS by intensity in water solution (c); hydrodynamic diameter of single macromolecules dissolved in water and MEK (d). Error bars for some points on the graphs are not seen because they are smaller than the symbol size.

increasing OEGMA fraction (Figure 3b). Specifically, addition of OEGMA monomeric units decreases the contact angle to up to 30°, whereas LMA addition increases the WCA to as high as 100° . It is obvious that for copolymers containing all three monomeric units, the contact angle can be tuned between 30° and 100° . For example, for the grafted film made of the $P(G_{15^{-}}O_{66^{-}}L_{19})$ copolymer, the WCA is equal to 74° . Using the WCA values derived from this experiment and assuming that the HCA is effectively zero, the surface energy of the coatings can be calculated (Supporting Information: S7). So As shown in

Figure 3a,b, the surface energy values for the grafted films range from 27 up to 62 mJ m⁻². the terpolymer $P(G_{15}-O_{66}-L_{19})$ has a surface energy of 36.4 mJ m⁻². The obtained results demonstrate the tunability of the resulting properties of the copolymer coatings.

Water Solubility and Grafting from Solution. The copolymers reported in this work can be anchored to colloidal objects from solution as well. In this method of surface modification, the copolymer solution is added to a colloidal suspension first. After the grafting, the colloidal objects are evacuated by centrifugation and redispersed in a fresh solvent. Although the surface modification with the copolymers can be conducted from a number of solvents, we were most interested in the grafting from water as a preferred solvent for biomedical applications and from ecological points of view. Therefore, we evaluated the water solubility of the copolymers containing OEGMA.

We found that the copolymers could be transferred to water from MEK solution and dissolved as individual chains and/or as macromolecular aggregates. The DLS studies showed that increasing OEGMA content leads to progressively better water solubility as the intensity of the DLS peaks related to single molecules rather than aggregates increases (Figure 3c). $P(G_{85}$ -O₁₅) with low OEGMA fraction leaves undispersed flakes in concentrated water solutions. Moreover, as indicated by the comparison of the hydrodynamic diameters (Figure 3d), this polymer has more affinity to MEK rather than the water as the size of the coil is larger in this organic solvent. 46 The P(GMA-OEGMA) copolymers with higher OEGMA content have excellent compatibility with water as they show higher tendency to dissolve as single molecules and have a high chain expansion parameter (larger size of the polymer coil) in water (Figure 3d). The terpolymer $P(G_{15}-O_{66}-L_{19})$ containing all three monomers (GMA-OEGMA-LMA) is soluble in water as well. The increase of the hydrodynamic diameter of the terpolymer macromolecules from 73 \pm 9 nm in MEK to 167 \pm 32 nm in water clearly indicated significant affinity of the copolymer to water. 46 The ability of the P(GMA-OEGMA-LMA) copolymer (containing hydrophobic LMA) to dissolve in water is essential to the process of surface modification as it opens venues to reduce the use of potentially environmentally hazardous solvents. In our next step, we demonstrated the ability of copolymers to be grafted to a colloidal object from water using GO as an example.

Grafting to GO. GO micron-scale sheets are used to fabricate ultrathin and transparent highly conductive graphenebased layers because GO serves as a "precursor" for its electrically conductive derivative, rGO. 37,51-56 GO possesses several advantages over pristine graphene from the manufacturing point of view: It is inexpensive and can be produced on a large scale from readily available graphite.³⁸ In addition, GO has excellent dispersibility in polar solvents including water⁵⁷ and its surface can be straightforwardly modified.⁵⁸ Therefore, GO has extreme adaptability and compatibility with various liquid media and solid substrates, which are important for employment of standard methods of layer nanomanufacturing.⁵⁹

The process of GO modification using water solution of $P(G_{34}-O_{66})$ and $P(G_{15}-O_{66}-L_{19})$ molecular brushes has been investigated with TGA (Supporting Information: Figure S7). We determined that, indeed, the molecular brushes could be readily grafted to the GO surface through the reactions of epoxy functional groups with (hydroxyl, carboxy, and epoxy) functional groups located on the GO surface. The resulting

kinetic isotherms are presented in Figure 4a,b. Specifically, we found that after the first 20 min, the grafted copolymer weight

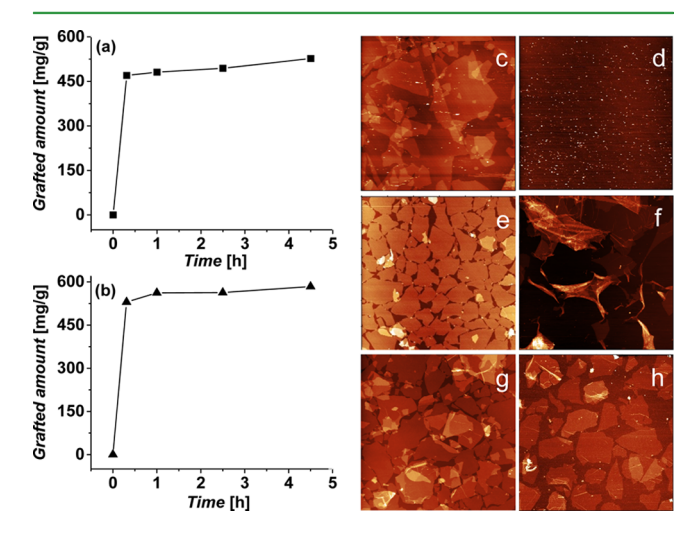


Figure 4. Grafted amount of molecular brushes to GO from water as a function of time: (a) $P(G_{66}-O_{34})$ and (b) $P(G_{15}-O_{66}-L_{19})$. AFM of pristine GO deposited on hydrophilic (c) and hydrophobic (d) surfaces, GO/P(G₆₆-O₃₄) on hydrophilic (e) and hydrophobic (f) surfaces, and GO/P(G₁₅-O₆₆-L₁₉) on hydrophilic (g) and hydrophobic (h) surfaces. The size of the scans is $30 \times 30 \ \mu \text{m}^2$, and vertical scale is 30 nm (c), 2 nm (d), 10 nm (e,g,h), and 70 nm (f). GO was deposited by dip-coating from water.

content was equal to 47% for $P(G_{34}-O_{66})$ and 53% for $P(G_{15}-O_{66})$ O_{66} - L_{19}), which increased up to 52% for $P(G_{34}$ - $O_{66})$ and 58% for P(G₁₅-O₆₆-L₁₉) after 4.5 h. This suggests that the grafting process is quite fast at the initial stage, similar to what is observed for the melt grafting. AFM has been used to determine the thickness of individual GO sheets modified with $P(G_{34}-O_{66})$ and $P(G_{15}-O_{66}-L_{19})$ (Supporting Information: S9). Cross-sectional analysis revealed that the thickness of the pristine GO sheet increased roughly by 1.5 nm for both P(G₃₄- O_{66}) and $P(G_{15}-O_{66}-L_{19})$. It confirmed that the molecular brush layer was indeed anchored to GO sheets.

We found that the grafting of the molecular brushes to the GO surface allows the formation of GO monolayers on surfaces of various polarities via dip-coating from water. In our initial experiments with pristine (unmodified with the copolymers) GO sheets, we found that it was impossible to obtain a GO dense monolayer via dip-coating on hydrophilic or hydrophobic surfaces. For hydrophilic surfaces (Figure 4c), we obtained either scarce coverage (40-50%) in the first layer or random multilayered/aggregated deposition with local wrinkles when the concentration of the GO suspension was increased. For hydrophobic surfaces, no GO deposition by dip-coating from water was observed (Figure 4d). In contrast, individual GO/ $P(G_{34}-O_{66})$ sheets were uniformly distributed on the surface of hydrophilic surface of silicon wafer (Figure 4e). However, the image presented in Figure 4f reveals that deposition of GO/ $P(G_{34}-O_{66})$ on the hydrophobic silicon wafer surface resulted in nonuniform coverage and crumpling of GO flakes. We associate this observation with poor adhesion of OEGMA units to the hydrophobic surface and capillary forces from fast solvent evaporation. 61,62 Conversely, by using the more hydrophobic P(G₁₅-O₆₆-L₁₉) molecular brush, it was possible to achieve the formation of uniform layers on both hydrophilic and hydrophobic surfaces (Figure 4g,h, respectively). Therefore, by

selecting an appropriate molecular brush for the modification of GO, it is possible to tune its compatibility with the surfaces of drastically different surface energies ranging from highly hydrophilic to highly hydrophobic.

Control of the Cell Adhesion with the Grafted Layers. Considering the unique properties, tunability, and versatility of the molecular brushes studied herein, multiple applications of the material can be envisioned. For instance, it can be used as a bioactive coating for medical devices. As was mentioned before, the hydrophilic and hydrophobic properties of the molecular brush can be precisely controlled by changing the ratio between the monomers constituting the molecular brush. Interactions of the human body with an implant are largely determined by the level of hydrophobicity of its surface. 63 In particular, it was shown that numerous processes, including protein adsorption, cell adhesion, and osseointegration, occur more likely on moderately hydrophobic surfaces.⁶⁴ On the other hand, a large body of evidence suggests that the use of the surfaces with pronounced hydrophilic properties completely eliminates protein adsorption and, therefore, prevents cell adhesion. With this in mind, in the present work, we hypothesized that cell attachment to the polymeric coating can be controlled by tuning the ratio between the components in the copolymers.

To demonstrate the applicability of molecular brush coating for the control over the biological processes, we have focused our research on the osteoblast attachment. The clinical implication for controlling osteoblast adhesion and spreading is of critical importance. 65 Many orthopedic implants are made of titanium, cobalt chromium, and stainless steel, which are relatively biologically inert materials. Some implants, especially those used in joint replacement, rely on osseous integration (bone growth directly onto or into the implant surface) to provide the proper functioning of the implant and withstand repetitive mechanical stress, while walking.⁶⁶ Once osteoblasts adhered to the implant surface, an enhanced proliferation, production of extracellular matrix, and mineralization occur. Therefore, there is a specific interest in bioactive coatings that can be deposited onto implants to enhance osteoblast adhesion and at the same time decrease bacterial adhesion to reduce the risk of infection.

Bioactive coatings must resist sheer stress, prevent bacterial adherence, and be both osteoinductive and osteoconductive. os Osteoinductive materials help to recruit local stem cells and induce osteogenesis, whereas osteoconductive materials promote osteoblast differentiation and proliferation. In another scenario, surgeons might wish to prevent osteoblast adherence because some implants are to be taken out within a few weeks to months from the patient's body. Such examples are Kirschner wires or external fixation pins used to help with deformity correction or temporarily stabilize fractures or arthrodesis. 69 Usually, these implants interact with both the internal and external environments. Therefore, an implant is needed that can withstand bacterial adherence to prevent infection (because it is interacting with the environment) while preventing local on-growth of osteoblasts so that it may be easily removed in the outpatient setting.⁷⁰ Polymer coatings on implants provide a unique opportunity to regulate the internal and external environments of the implant to ensure surgical

To demonstrate the ability to tune cell adhesion by the grafted copolymer layers, mouse osteoblasts were cultured in the presence of silicon wafers coated with the PGMA homopolymer, $P(G_{26}-L_{74})$, $P(G_{15}-O_{66}-L_{19})$, and $P(G_{34}-O_{66})$

molecular brushes. Cells were allowed to adhere to the surfaces; osteoblast attachment was assessed by means of SEM (Figure 5) and the LIVE/DEAD assay (Figure 6). The SEM studies

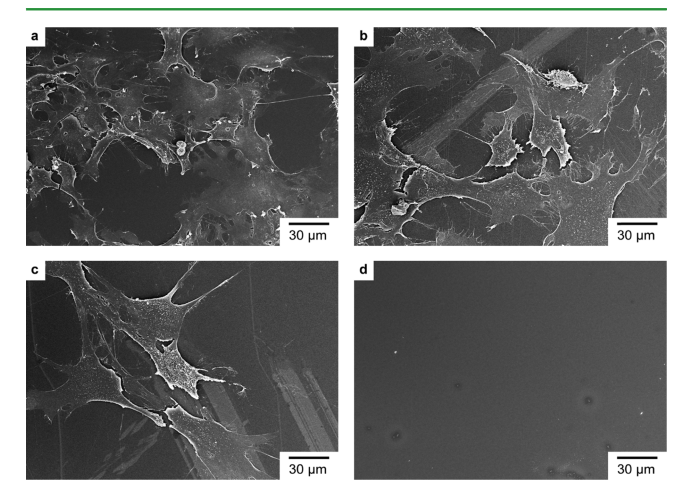


Figure 5. Scanning electron micrographs of the osteoblasts attached to the silicon wafers coated with (a) PGMA, (b) $P(G_{26}-L_{74})$, (c) $P(G_{15}-O_{66}-L_{19})$, and (d) $P(G_{66}-O_{34})$.

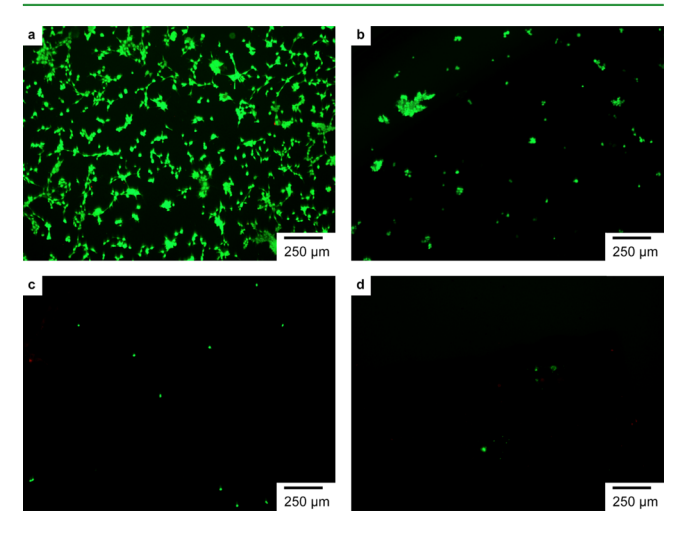


Figure 6. Fluorescent microscopy images of the osteoblasts attached to the silicon wafers coated with (a) PGMA, (b) $P(G_{26}\text{-}L_{74})$, (c) $P(G_{15}\text{-}O_{66}\text{-}L_{19})$, and (d) $P(G_{66}\text{-}O_{34})$. The cells were stained with calcein AM and EthD-1 prior to visualization. Osteoblasts stained green are viable, whereas those stained red are dead.

revealed different levels of cell adhesion and protein adsorption to the polymeric coatings. The osteoblast attachment and spreading was shown for PGMA and $P(G_{26}\text{-}L_{74})$ coatings. At the same time, little to no evidence of cell adhesion was observed for the $P(G_{34}\text{-}O_{66})$ coating (Figure 5d). Moreover, in the latter case, the surface of the sample was found to repel proteins, in contrast to the PGMA and $P(G_{26}\text{-}L_{74})$ coatings. These samples appeared to be covered with thick and developed layers of proteins that are, apparently, secreted by attached osteoblasts. The $P(G_{15}\text{-}O_{66}\text{-}L_{19})$ coating represents a very important intermediate case: although osteoblast attachment was evident from the images and the cells exhibited conventional morphology, no proteins were adsorbed on the surface

Proteins tend to have high affinity toward hydrophobic surfaces, facilitating cell adhesion and spreading. Considering the hydrophobic nature of PGMA and P(G₂₆-L₇₄) coatings, the obtained results were obvious. At the same time, it is wellknown that PEGylated surfaces possess strong protein- and, as a result, cell-repulsive properties. Therefore, no adhesion of osteoblasts on the $P(G_{34}-O_{66})$ coating is, apparently, due to the high percentage of PEG-containing components. Because the $P(G_{15}-O_{66}-L_{19})$ system exhibited lower content of PEG, osteoblasts were able to adhere and spread across the surface. However, because of the low work of adhesion, this system was still demonstrating protein-repulsive properties.

The LIVE/DEAD assay was also used to assess the number and viability of osteoblasts attached to the polymeric coatings. The results are presented in Figure 6. These images confirmed the results of SEM and revealed a large number of cells attached to the PGMA and P(G₂₆-L₇₄) coatings, whereas only a few osteoblasts adhered to the surface of the $P(G_{34}\text{-}O_{66})$ samples. In the case of the $P(G_{15}-O_{66}-L_{19})$ coating, the number of cells lodging the sample was higher than that for P(G₃₄-O₆₆). However, compared to PGMA and P(G₂₆-L₇₄) coatings, the P(G₁₅-O₆₆-L₁₉) polymer system exhibited significantly less adherent cells, demonstrating moderate cell-repulsive properties. It is important to emphasize that all four polymer systems demonstrated high biocompatibility and low cytotoxicity, resulting in little to no evidence of nonviable osteoblasts attached to the samples. We also conducted the standard MTT assay to evaluate the effect of the PGMA and $(P(G_{34}-O_{66}))$ coatings on the osteoblast proliferation rate (Supporting Information: S10 and Figure S9). The results confirmed that the systems we studied show no signs of cytotoxicity. In general, our work has demonstrated that poly(GMA-ran-OEGMA-ran-LMA)-based coatings offer high variability of their cell adhesion properties achieved through the one-step process of deposition and annealing.

CONCLUSIONS

We have demonstrated that functional grafted polymer layers can be deposited from aqueous solutions or with minimal use of solvents, using reactive statistical molecular brushes made of GMA, OEGMA, and LMA. As an example of the molecular brush applications, we showed the ability to control the deposition of GO sheets on both hydrophilic and hydrophobic surfaces using GO modified with P(G₃₄-O₆₆) and/or P(G₁₅-O₆₆-L₁₉) molecular brushes. Also, the ability to tune the osteoblast cell adhesion with the molecular brush-based coatings was established. Considering the high biocompatibility and low cytotoxicity of the copolymers, there are obvious opportunities for P(GMA-OEGMA-LMA) usage in biomedical applications. In general, these molecular brushes are a flexible tool for surface modification, which has minimal requirements for the substrate and can be applied in a controllable fashion through a straightforward procedure. The use of the highly branched reactive macromolecules in grafting modification allows anchoring a significant number of functional moieties via one-step grafting-to attachment.

ASSOCIATED CONTENT

Supporting Information

The Supporting Information is available free of charge on the ACS Publications website at DOI: 10.1021/acsami.7b19815.

> Calculation of the reactivity ratios; synthesis of GMA-OEGMA-LMA terpolymers; parameters of the brushlike copolymers; FTIR spectra of P(GMA-OEGMA) and

P(GMA-LMA); measurement of the degree of polymerization and molecular weight; thermal properties of the copolymers; estimation of surface energy of the grafted copolymer films; TGA data for GO modification; AFM of GO monolayer; MTT assay results; sequence length distribution for $P(G_{34}-O_{66})$ and $P(G_{26}-L_{74})$ copolymers; FTIR analysis of epoxy groups consumption during copolymer grafting; and references (PDF)

AUTHOR INFORMATION

Corresponding Author

*E-mail: luzinov@clemson.edu.

ORCID ®

Nikolay Borodinov: 0000-0002-8562-5629 Nataraja Sekhar Yadavalli: 0000-0001-7849-8900 Vladimir V. Tsukruk: 0000-0001-5489-0967

Sergiv Minko: 0000-0002-7747-9668 Igor Luzinov: 0000-0002-1604-6519

Notes

The authors declare no competing financial interest.

ACKNOWLEDGMENTS

This work was supported by the National Science Foundation via CMMI 1538215 and EPSCoR OIA 1655740 awards. The authors thank Kimberly Ivey (Clemson University) for assistance with DSC and TGA measurements.

REFERENCES

- (1) Stuart, M. A. C.; Huck, W. T. S.; Genzer, J.; Müller, M.; Ober, C.; Stamm, M.; Sukhorukov, G. B.; Szleifer, I.; Tsukruk, V. V.; Urban, M.; Winnik, F.; Zauscher, S.; Luzinov, I.; Minko, S. Emerging Applications of Stimuli-Responsive Polymer Materials. Nat. Mater. 2010, 9, 101-
- (2) Luzinov, I.; Minko, S.; Tsukruk, V. V. Adaptive and Responsive Surfaces through Controlled Reorganization of Interfacial Polymer Layers. Prog. Polym. Sci. 2004, 29, 635-698.
- (3) Liu, Y.; Klep, V.; Luzinov, I. To Patterned Binary Polymer Brushes via Capillary Force Lithography and Surface-Initiated Polymerization. J. Am. Chem. Soc. 2006, 128, 8106-8107.
- (4) Olivier, A.; Meyer, F.; Raquez, J.-M.; Damman, P.; Dubois, P. Surface-Initiated Controlled Polymerization as a Convenient Method for Designing Functional Polymer Brushes: From Self-Assembled Monolayers to Patterned Surfaces. Prog. Polym. Sci. 2012, 37, 157-181.
- (5) Lokitz, B. S.; Messman, J. M.; Hinestrosa, J. P.; Alonzo, J.; Verduzco, R.; Brown, R. H.; Osa, M.; Ankner, J. F.; Kilbey, S. M. Dilute Solution Properties and Surface Attachment of RAFT Polymerized 2-Vinyl-4,4-dimethyl Azlactone (VDMA). Macromolecules 2009, 42, 9018-9026.
- (6) Zhao, B.; Brittain, W. J. Polymer Brushes: Surface-Immobilized Macromolecules. Prog. Polym. Sci. 2000, 25, 677-710.
- (7) Keating, J. J.; Imbrogno, J.; Belfort, G. Polymer Brushes for Membrane Separations: A Review. ACS Appl. Mater. Interfaces 2016, 8,
- (8) Zoppe, J. O.; Ataman, N. C.; Mocny, P.; Wang, J.; Moraes, J.; Klok, H.-A. Surface-Initiated Controlled Radical Polymerization: Stateof-the-Art, Opportunities, and Challenges in Surface and Interface Engineering with Polymer Brushes. Chem. Rev. 2017, 117, 1105-1318.
- (9) Zdyrko, B.; Luzinov, I. Polymer Brushes by the "Grafting to" Method. Macromol. Rapid Commun. 2011, 32, 859-869.
- (10) Kamperman, M.; Synytska, A. Switchable Adhesion by Chemical Functionality and Topography. J. Mater. Chem. 2012, 22, 19390-19401.

- (11) Luzinov, I.; Minko, S.; Tsukruk, V. V. Responsive Brush Layers: from Tailored Gradients to Reversibly Assembled Nanoparticles. Soft Matter 2008, 4, 714-725.
- (12) Panyukov, S.; Zhulina, E. B.; Sheiko, S. S.; Randall, G. C.; Brock, J.; Rubinstein, M. Tension Amplification in Molecular Brushes in Solutions and on Substrates. J. Phys. Chem. B 2009, 113, 3750-3768.
- (13) Panyukov, S. V.; Sheiko, S. S.; Rubinstein, M. Amplification of Tension in Branched Macromolecules. Phys. Rev. Lett. 2009, 102,
- (14) Paturej, J.; Sheiko, S. S.; Panyukov, S.; Rubinstein, M. Molecular Structure of Bottlebrush Polymers in Melts. Sci. Adv. 2016, 2, e1601478.
- (15) Daniel, W. F. M.; Burdyńska, J.; Vatankhah-Varnoosfaderani, M.; Matyjaszewski, K.; Paturej, J.; Rubinstein, M.; Dobrynin, A. V.; Sheiko, S. S. Solvent-free, Supersoft and Superelastic Bottlebrush Melts and Networks. Nat. Mater. 2016, 15, 183-189.
- (16) Hu, J.; Wang, G.; Zhao, W.; Liu, X.; Zhang, L.; Gao, W. Site-Specific In Situ Growth of an Interferon-Polymer Conjugate that Outperforms PEGASYS in Cancer Therapy. Biomaterials 2016, 96,
- (17) Smeets, N. M. B.; Patenaude, M.; Kinio, D.; Yavitt, F. M.; Bakaic, E.; Yang, F.-C.; Rheinstädter, M.; Hoare, T. Injectable Hydrogels with in Situ-Forming Hydrophobic Domains: Oligo(D,L-Lactide) Modified Poly(Oligoethylene Glycol Methacrylate) Hydrogels. Polym. Chem. 2014, 5, 6811-6823.
- (18) Shi, X.; Wang, Y.; Li, D.; Yuan, L.; Zhou, F.; Wang, Y.; Song, B.; Wu, Z.; Chen, H.; Brash, J. L. Cell Adhesion on a POEGMA-Modified Topographical Surface. Langmuir 2012, 28, 17011-17018.
- (19) Liu, M.; Leroux, J.-C.; Gauthier, M. A. Conformation-Function Relationships for the Comb-Shaped Polymer pOEGMA. Prog. Polym. Sci. 2015, 48, 111-121.
- (20) Skandalis, A.; Pispas, S. PLMA-b-POEGMA Amphiphilic Block Copolymers: Synthesis and Self-Assembly in Aqueous Media. J. Polym. Sci., Part A: Polym. Chem. 2017, 55, 155-163.
- (21) Wang, G.; Chen, M.; Guo, S.; Hu, A. Synthesis, Self-Assembly, and Thermosensitivity of Amphiphilic POEGMA-PDMS-POEGMA Triblock Copolymers. J. Polym. Sci., Part A: Polym. Chem. 2014, 52, 2684-2691.
- (22) Knop, K.; Pretzel, D.; Urbanek, A.; Rudolph, T.; Scharf, D. H.; Schallon, A.; Wagner, M.; Schubert, S.; Kiehntopf, M.; Brakhage, A. A.; Schacher, F. H.; Schubert, U. S. Star-Shaped Drug Carriers for Doxorubicin with POEGMA and POETOXMA Brush-Like Shells: A Structural, Physical, and Biological Comparison. Biomacromolecules 2013, 14, 2536-2548.
- (23) Lin, P. T.; Giammarco, J.; Borodinov, N.; Savchak, M.; Singh, V.; Kimerling, L. C.; Tan, D. T. H.; Richardson, K. a.; Luzinov, I.; Agarwal, A. Label-Free Water Sensors Using Hybrid Polymer-Dielectric Mid-Infrared Optical Waveguides. ACS Appl. Mater. Interfaces 2015, 7, 11189-11194.
- (24) Borodinov, N.; Soliani, A. P.; Galabura, Y.; Zdyrko, B.; Tysinger, C.; Novak, S.; Du, Q.; Huang, Y.; Singh, V.; Han, Z.; Hu, J.; Kimerling, L.; Agarwal, A. M.; Richardson, K.; Luzinov, I. Gradient Polymer Nanofoams for Encrypted Recording of Chemical Events. ACS Nano **2016**, 10, 10716-10725.
- (25) Hoy, O.; Zdyrko, B.; Lupitskyy, R.; Sheparovych, R.; Aulich, D.; Wang, J.; Bittrich, E.; Eichhorn, K.-J.; Uhlmann, P.; Hinrichs, K.; Müller, M.; Stamm, M.; Minko, S.; Luzinov, I. Synthetic Hydrophilic Materials with Tunable Strength and a Range of Hydrophobic Interactions. Adv. Funct. Mater. 2010, 20, 2240-2247.
- (26) Zdyrko, B.; Klep, V.; Li, X.; Kang, Q.; Minko, S.; Wen, X.; Luzinov, I. Polymer Brushes as Active Nanolayers for Tunable Bacteria Adhesion. Mater. Sci. Eng., C 2009, 29, 680-684.
- (27) Zdyrko, B.; Hoy, O.; Kinnan, M. K.; Chumanov, G.; Luzinov, I. Nano-Patterning with Polymer Brushes via Solvent-Assisted Polymer Grafting. Soft Matter 2008, 4, 2213-2219.
- (28) Borodinov, N.; Giammarco, J.; Patel, N.; Agarwal, A.; O'Donnell, K. R.; Kucera, C. J.; Jacobsohn, L. G.; Luzinov, I. Stability of Grafted Polymer Nanoscale Films toward Gamma Irradiation. ACS Appl. Mater. Interfaces 2015, 7, 19455-19465.

- (29) Soto-Cantu, E.; Lokitz, B. S.; Hinestrosa, J. P.; Deodhar, C.; Messman, J. M.; Ankner, J. F.; Kilbey, S. M. Versatility of Alkyne-Modified Poly(Glycidyl Methacrylate) Layers for Click Reactions. Langmuir 2011, 27, 5986-5996.
- (30) Benaglia, M.; Alberti, A.; Giorgini, L.; Magnoni, F.; Tozzi, S. Poly(glycidyl methacrylate): A Highly Versatile Polymeric Building Block for Post-Polymerization Modifications. Polym. Chem. 2013, 4,
- (31) Safa, K. D.; Nasirtabrizi, M. H. One-Pot, Novel Chemical Modification of Glycidyl Methacrylate Copolymers with Very Bulky Organosilicon Side Chain Substituents. Eur. Polym. J. 2005, 41, 2310-
- (32) Galabura, Y.; Soliani, A. P.; Giammarco, J.; Zdyrko, B.; Luzinov, I. Temperature Controlled Shape Change of Grafted Nanofoams. Soft Matter 2014, 10, 2567-2573.
- (33) Scheibe, P.; Barz, M.; Hemmelmann, M.; Zentel, R. Langmuir-Blodgett Films of Biocompatible Poly(HPMA)-block-poly(lauryl methacrylate) and Poly(HPMA)-random-poly(lauryl methacrylate): Influence of Polymer Structure on Membrane Formation and Stability. Langmuir 2010, 26, 5661-5669.
- (34) Feng, Y.; Xiao, C. F. Research on Butyl Methacrylate-Lauryl Methacrylate Copolymeric Fibers for Oil Absorbency. J. Appl. Polym. Sci. 2006, 101, 1248-1251.
- (35) Chatterjee, D. P.; Mandal, B. M. Triblock Thermoplastic Elastomers with Poly(lauryl methacrylate) as the Center Block and Poly(methyl methacrylate) or Poly(tert-butyl methacrylate) as End Blocks. Morphology and Thermomechanical Properties. Macromolecules 2006, 39, 9192-9200.
- (36) Yadavalli, N. S.; Borodinov, N.; Choudhury, C. K.; Quiñones-Ruiz, T.; Laradji, A. M.; Tu, S.; Lednev, I. K.; Kuksenok, O.; Luzinov, I.; Minko, S. Thermal Stabilization of Enzymes with Molecular Brushes. ACS Catal. 2017, 7, 8675-8684.
- (37) Savchak, M.; Borodinov, N.; Burtovyy, R.; Anayee, M.; Hu, K.; Ma, R.; Grant, A.; Li, H.; Cutshall, D. B.; Wen, Y.; Koley, G.; Harrell, W. R.; Chumanov, G.; Tsukruk, V.; Luzinov, I. Highly Conductive and Transparent Reduced Graphene Oxide Nanoscale Films via Thermal Conversion of Polymer-Encapsulated Graphene Oxide Sheets. ACS Appl. Mater. Interfaces 2018, 10, 3975-3985.
- (38) Hummers, W. S.; Offeman, R. E. Preparation of Graphitic Oxide. J. Am. Chem. Soc. 1958, 80, 1339.
- (39) Luzinov, I.; Julthongpiput, D.; Liebmann-Vinson, A.; Cregger, T.; Foster, M. D.; Tsukruk, V. V. Epoxy-Terminated Self-Assembled Monolayers: Molecular Glues for Polymer Layers. Langmuir 2000, 16, 504-516.
- (40) Odian, G. G. Principles of Polymerization; Wiley-Interscience: Hoboken, NJ, 2004.
- (41) Driva, P.; Bexis, P.; Pitsikalis, M. Radical Copolymerization of 2vinyl pyridine and Oligo(Ethylene Glycol) Methyl Ether Methacrylates: Monomer Reactivity Ratios and Thermal Properties. Eur. Polym. *J.* **2011**, *47*, 762–771.
- (42) Ito, K.; Tanaka, K.; Tanaka, H.; Imai, G.; Kawaguchi, S.; Itsuno, S. Poly(ethylene oxide) Macromonomers. 7. Micellar Polymerization in Water. Macromolecules 1991, 24, 2348-2354.
- (43) Yamamoto, T. Normal Mode Analysis of The Conformational Fluctuation of Polymethylene Chains in their Nearly Extended States. J. Chem. Phys. 1991, 95, 7717-7725.
- (44) Rubinstein, M.; Colby, R. H. Polymer Physics; Oxford University Press: Oxford, 2003; p 442.
- (45) Raczek, J. Examples of the Determination of Molecular-Weight Distributions by Dynamic Light-Scattering. Eur. Polym. J. 1982, 18,
- (46) Sperling, L. H. Introduction to Physical Polymer Science, 4th ed.; Wiley-Interscience Hoboken: New Jersey, 2006; Chapter 5, p 845.
- (47) Hempel, E.; Huth, H.; Beiner, M. Interrelation Between Side Chain Crystallization and Dynamic Glass Transitions in Higher Poly(N-Alkyl Methacrylates). Thermochim. Acta 2003, 403, 105-114.
- (48) Floudas, G.; Placke, P.; Stepanek, P.; Brown, W.; Fytas, G.; Ngai, K. L. Dynamics of the "Strong" Polymer of n-Lauryl

- Methacrylate Below and Above the Glass Transition. *Macromolecules* **1995**, 28, 6799–6807.
- (49) Burtovyy, O.; Klep, V.; Chen, H.-C.; Hu, R.-K.; Lin, C.-C.; Luzinov, I. Hydrophobic Modification of Polymer Surfaces via "Grafting to" Approach. J. Polym. Sci., Part B: Polym. Phys. 2007, 46, 137–154.
- (50) Luzinova, Y.; Zdyrko, B.; Luzinov, I.; Mizaikoff, B. In Situ Trace Analysis of Oil in Water with Mid-Infrared Fiberoptic Chemical Sensors. *Anal. Chem.* **2012**, *84*, 1274–1280.
- (51) Garg, R.; Elmas, S.; Nann, T.; Andersson, M. R. Deposition Methods of Graphene as Electrode Material for Organic Solar Cells. *Adv. Energy Mater.* **2017**, *7*, 1601393.
- (52) Ferrari, A. C.; Bonaccorso, F.; Fal'ko, V.; Novoselov, K. S.; Roche, S.; Bøggild, P.; Borini, S.; Koppens, F. H. L.; Palermo, V.; Pugno, N.; Garrido, J. A.; Sordan, R.; Bianco, A.; Ballerini, L.; Prato, M.; Lidorikis, E.; Kivioja, J.; Marinelli, C.; Ryhänen, T.; Morpurgo, A.; Coleman, J. N.; Nicolosi, V.; Colombo, L.; Fert, A.; Garcia-Hernandez, M.; Bachtold, A.; Schneider, G. F.; Guinea, F.; Dekker, C.; Barbone, M.; Sun, Z.; Galiotis, C.; Grigorenko, A. N.; Konstantatos, G.; Kis, A.; Katsnelson, M.; Vandersypen, L.; Loiseau, A.; Morandi, V.; Neumaier, D.; Treossi, E.; Pellegrini, V.; Polini, M.; Tredicucci, A.; Williams, G. M.; Hong, B. H.; Ahn, J.-H.; Kim, J. M.; Zirath, H.; van Wees, B. J.; van der Zant, H.; Occhipinti, L.; Di Matteo, A.; Kinloch, I. A.; Seyller, T.; Quesnel, E.; Feng, X.; Teo, K.; Rupesinghe, N.; Hakonen, P.; Neil, S. R. T.; Tannock, Q.; Löfwander, T.; Kinaret, J. Science and Technology Roadmap for Graphene, Related Two-Dimensional Crystals, and Hybrid Systems. *Nanoscale* 2015, 7, 4598–4810.
- (53) Pang, S.; Hernandez, Y.; Feng, X.; Müllen, K. Graphene as Transparent Electrode Material for Organic Electronics. *Adv. Mater.* **2011**, 23, 2779–2795.
- (54) Zheng, Q.; Li, Z.; Yang, J.; Kim, J.-K. Graphene Oxide-Based Transparent Conductive Films. *Prog. Mater. Sci.* **2014**, *64*, 200–247.
- (55) Huang, X.; Yin, Z.; Wu, S.; Qi, X.; He, Q.; Zhang, Q.; Yan, Q.; Boey, F.; Zhang, H. Graphene-Based Materials: Synthesis, Characterization, Properties, and Applications. *Small* **2011**, *7*, 1876–1902.
- (56) López-Naranjo, E. J.; González-Ortiz, L. J.; Apátiga, L. M.; Rivera-Muñoz, E. M.; Manzano-Ramírez, A. Transparent Electrodes: A Review of the Use of Carbon-Based Nanomaterials. *J. Nanomater.* **2016**, 2016, 4928365.
- (57) Stankovich, S.; Dikin, D. A.; Piner, R. D.; Kohlhaas, K. A.; Kleinhammes, A.; Jia, Y.; Wu, Y.; Nguyen, S. T.; Ruoff, R. S. Synthesis of Graphene-Based Nanosheets via Chemical Reduction of Exfoliated Graphite Oxide. *Carbon* **2007**, *45*, 1558–1565.
- (\$\frac{1}{2}\$) Layek, R. K.; Nandi, A. K. A Review on Synthesis and Properties of Polymer Functionalized Graphene. *Polymer* **2013**, *54*, 5087–5103.
- (59) Shao, J.-J.; Lv, W.; Yang, Q.-H. Self-Assembly of Graphene Oxide at Interfaces. *Adv. Mater.* **2014**, *26*, 5586–5612.
- (60) Wang, X.; Zhi, L.; Müllen, K. Transparent, Conductive Graphene Electrodes for Dye-Sensitized Solar Cells. *Nano Lett.* **2008**, *8*, 323–327.
- (61) Wang, W.-N.; Jiang, Y.; Biswas, P. Evaporation-Induced Crumpling of Graphene Oxide Nanosheets in Aerosolized Droplets: Confinement Force Relationship. *J. Phys. Chem. Lett.* **2012**, *3*, 3228–3233.
- (62) Becton, M.; Zhang, L.; Wang, X. Mechanics of Graphyne Crumpling. Phys. Chem. Chem. Phys. 2014, 16, 18233–18240.
- (63) Anderson, J. M.; Rodriguez, A.; Chang, D. T. Foreign Body Reaction to Biomaterials. *Semin. Immunol.* **2008**, 20, 86–100.
- (64) Dee, K. C.; Puleo, D. A.; Bizios, R. An Introduction to Tissue-biomaterial Interactions; Wiley-Liss, Inc: New York, 2002.
- (65) Anselme, K. Osteoblast Adhesion on Biomaterials. *Biomaterials* **2000**, 21, 667–681.
- (66) Albrektsson, T.; Johansson, C. Osteoinduction, Osteoconduction and Osseointegration. Eur. Spine J. 2001, 10, S96-S101.
- (67) Lyndon, J. A.; Boyd, B. J.; Birbilis, N. Metallic Implant Drug/Device Combinations for Controlled Drug Release in Orthopaedic Applications. *J. Controlled Release* **2014**, *179*, 63–75.
- (68) Beardmore, A. A.; Brooks, D. E.; Wenke, J. C.; Thomas, D. B. Effectiveness of Local Antibiotic Delivery with an Osteoinductive and

- Osteoconductive Bone-Graft Substitute. J. Bone Jt. Surg. Am. Vol. 2005, 87, 107–112.
- (69) Albrektsson, T.; Albrektsson, B. Osseointegration of Bone Implants: A Review of an Alternative Mode of Fixation. *Acta Orthop. Scand.* **1987**, *58*, *567*–*577*.
- (70) Goodman, S. B.; Yao, Z.; Keeney, M.; Yang, F. The Future of Biologic Coatings for Orthopaedic Implants. *Biomaterials* **2013**, *34*, 3174–3183.